Adipose differentiation-related protein knockdown inhibits vascular smooth muscle cell proliferation and migration and attenuates neointima formation

HAOMIN ZHAO, TAO HAN, XIN HONG and DAJUN SUN

Department of Vascular Surgery, China-Japan Union Hospital of Jilin University, Changchun, Jilin 130033, P.R. China

Abstract. Vascular smooth muscle cells (VSMCs) have an important role in atherosclerosis development. Evidence has demonstrated that adipose differentiation-related protein (ADRP) is associated with foam cell formation and atherosclerosis progression. However, to the best of our knowledge, no previous studies have investigated the role of ADRP knockdown in platelet-derived growth factor (PDGF)-stimulated proliferation and migration of VSMCs *in vitro*. Furthermore, the effect of ADRP knockdown on neointima formation *in vivo* remains unclear. In the present study, primary human aortic VSMCs were incubated with PDGF following ADRP small interfering (si)RNA transfection. Cell viability, migration and cell cycle distribution were analyzed by MTT, wound healing and Transwell assays and flow cytometry, respectively. Extracellular signal-regulated kinase (ERK), phosphorylated (p)-ERK, Akt, p-Akt, proliferating cell nuclear antigen (PCNA), matrix metalloproteinase (MMP)-2 and MMP-9 protein levels were determined by western blotting. Apolipoprotein $E^{-/-}$ mice fed an atherogenic diet were injected with siADRP or control siRNA twice a week. After 3 weeks of therapy, aortas were excised and ADRP mRNA and protein expression was determined. Neointima formation was assessed by hematoxylin and eosin staining. The results of the current study demonstrated that ADRP knockdown significantly inhibited PDGF-induced increases in VSMC viability, caused G1 phase cell cycle arrest and decreased PCNA expression. Knockdown of ADRP inhibited PDGF-induced migration of VSMCs by reducing MMP protein expression and activity. In addition, the present study also demonstrated that ADRP knockdown inhibited ERK and Akt signaling pathways in response to PDGF. Furthermore, siADRP administration suppressed neointima formation in the mouse model. The results of the present study indicate that ADRP may be a potential target for the treatment of atherosclerosis.

Introduction

Atherosclerosis is a chronic inflammatory disease that contributes to cardiovascular disease, a leading cause of mortality (1). It is characterized by excessive lipid deposition in the arterial wall and atherosclerotic plaque formation (2,3). It causes insufficient blood supply to coronary arteries and myocardial ischemia, which are the pathological basis of coronary heart disease (4). The etiology of atherosclerosis is multifactorial and includes diabetes mellitus, hypertension, smoking, dyslipidemia and genetic factors (5,6). Atherosclerotic lesion formation starts with vascular endothelial cell injury, lipid deposition and abnormal proliferation of vascular smooth muscle cells (VSMCs) (7). During atherosclerosis progression, proliferation and migration of VSMCs from the media to intima contribute to intimal hyperplasia and vascular stenosis (8).

Adipose differentiation-related protein (ADRP), also termed perilipin 2 or adipophilin, is expressed in the majority of cell types and is commonly used as a lipid droplet marker (9). McIntosh *et al* (10) reported that ADRP interacts with lipids on the lipid droplet surface and regulates the levels of key enzymes and lipids that have critical roles in maintaining the structure and function of lipid droplets. ADRP is highly expressed in atherosclerotic plaques in humans (11). Xu *et al* (12) previously demonstrated that elevation of ADRP expression in human atherosclerotic plaques is closely associated with the instability of plaques, and Paul *et al* (13) demonstrated that ADRP deficiency protects apolipoprotein E (apoE)$^{-/-}$ mice against atherosclerosis by suppressing foam cell formation, which is a hallmark of atherosclerosis. However, the role of ADRP in the proliferation and migration of human VSMCs induced by platelet-derived growth factor (PDGF) *in vitro* and the effect of ADRP knockdown on neointima formation *in vivo* remains to be established.

Mitogen-activated protein kinases (MAPKs) are expressed in all types of cells (14). The MAPK family consists of multiple kinases, including p38 MAPK, c-Jun N-terminal kinase and extracellular signal-regulated kinase (ERK) (15). Protein kinase B (Akt) is a serine/threonine protein kinase, and Akt signaling is involved in cell proliferation, migration and tumor

Correspondence to: Dr Dajun Sun, Department of Vascular Surgery, China-Japan Union Hospital of Jilin University, 126 Xiantai Avenue, Changchun, Jilin 130033, P.R. China
E-mail: dajunsun_cc@tom.com

metastasis (16,17). Previous evidence has demonstrated that ERK and Akt signaling pathways participate in the regulation of VSMC proliferation and migration (16,18-20).

In the present study, ADRP knockdown was performed in primary human aortic VSMCs using small interfering (si)RNA. The cells were treated with PDGF following siRNA transfection. Subsequently, proliferation and migration of VSMCs were measured and the underlying mechanism was investigated. In addition, the present study investigated the effect of ADRP knockdown on atherosclerosis in apoE$^{-/-}$ mice.

Materials and methods

Cell culture. Primary human aortic VSMCs were purchased from CHI Scientific, Ltd. (Jiangyin, China) and cultured in Dulbecco's Modified Eagle's Medium (DMEM; Gibco; Thermo Fisher Scientific, Inc., Waltham, MA, USA) containing 15% fetal bovine serum (FBS; Hyclone; GE Healthcare Life Sciences, Logan, UT, USA) at 37˚C in a humidified atmosphere with 5% CO_2.

Transfection of siRNA. siRNA targeting ADRP and non-targeting siRNA (siCtr) were synthesized by Shanghai GenePharma Co., Ltd. (Shanghai, China). The sequences were as follows: siADRP, 5'-GAGACUGCCUAUUCUGAA UTT-3'; and siCtr, 5'-UUCUCCGAACGUGUCACGUTT-3'. VSMCs were seeded into 6-well plates ($4x10^5$ cells/well). After culturing for 23 h at 37˚C, the medium was replaced with serum-free DMEM and the cells were cultured for 1 h at 37˚C. Subsequently, Lipofectamine® 2000 Transfection reagent (Invitrogen; Thermo Fisher Scientific, Inc.) was used to transfect 100 pmol siADRP or siCtr into VSMCs. After 4 h, the culture medium was replaced by DMEM containing 15% FBS and cultured at 37˚C.

Cell viability. Cells were seeded into 96-well plates at a density of $3x10^3$ cells/well, cultured at 37˚C for 24 h and subsequently transfected with the siRNA as described. Twenty-four hours post-transfection, the cells were incubated with PDGF (10 ng/ml; PeproTech, Inc., Rocky Hill, NJ, USA) at 37˚C for 24, 48 and 72 h. The cells in the control group were cultured at 37˚C without any treatment. Subsequently, 5 mg/ml MTT reagent (Sigma-Aldrich; Merck KGaA, Darmstadt, Germany) was added into each well in 96-well plates and incubated for 4 h at 37˚C. To dissolve the formazan crystals, dimethylsulfoxide (Sigma-Aldrich; Merck KGaA) was added after removing the culture medium and the absorbance at 490 nm was measured using a microplate reader (BioTek Instruments, Inc., Winooski, VT, USA).

Flow cytometry analysis. After stimulating with 10 ng/ml PDGF for 48 h at 37˚C, the siRNA-transfected cells were fixed and permeabilized with 70% ethanol for 2 h at 4˚C and harvested by centrifugation at 550 x g for 5 min. For cell cycle analysis, the cells ($1-5x10^6$ cells) were incubated with RNase A at 37˚C for 30 min in a water bath and subsequently stained with propidium iodide staining solution (Wanleibio, Shenyang, China) at 4˚C for 30 min in the dark. Cell cycle distribution was analyzed by a BD Accuri C6 flow cytometer using Accuri C6 software (both from BD Biosciences, San Jose, CA, USA).

Wound healing assay. Cells were treated with PDGF for 48 h after siRNA transfection. Subsequently, the cells were cultured to ~90% confluence in serum-free DMEM containing 1 μg/ml mitomycin C (Sigma-Aldrich; Merck KGaA) at 37˚C for 1 h before they were subjected to wound healing assay. Briefly, a 200 μl pipette tip was used to scratch the cell layers. Subsequently, the wound was washed with serum-free medium and further cultured in serum-free medium for 0, 12 and 24 h at 37˚C. The cells were imaged under an inverted microscope (magnification, x100) (Motic Incorporation, Ltd., Causeway Bay, Hong Kong).

Migration assay. Cell migration ability was determined by Transwell migration assay. Briefly, cells in serum-free medium ($1x10^4$ cells) were added into each well in the upper chamber and DMEM containing 20% FBS was added into lower chamber. Subsequently, the chamber (Corning Incorporated, Corning, NY, USA) was cultured for 24 h at 37˚C. After washing with PBS, the non-migrated cells were removed by cotton swabs and the cells on the lower membrane were fixed with 4% paraformaldehyde (Sinopharm Chemical Reagent Co., Ltd., Shanghai, China) for 20 min at room temperature, stained with crystal violet (Amresco, LLC, Solon, OH, USA) and imaged under an inverted microscope (magnification, x200) (Motic Incorporation, Ltd.). The average numbers of migrated cells in five fields of view were calculated.

Gelatin zymography. The activities of matrix metalloproteinase (MMP)-2 and MMP-9 were examined by gelatin zymography. At 24 h after transfection, the cells were treated with PDGF for 24 h at 37˚C. The conditioned medium was collected and the protein concentration was quantified using a Bicinchoninic Acid assay kit (Wanleibio). Proteins (30 μg per lane) were subsequently separated by 10% SDS-PAGE containing gelatin (Sigma-Aldrich; Merck KGaA). The gels were washed twice for 40 min each in 2.5% Triton X-100 to remove the SDS, incubated with developing buffer for 40 h at 37˚C and stained for 3 h at room temperature with 0.05% Coomassie Brilliant Blue R-250 (Amresco, LLC). After three destaining washes in a mixture of methanol and acetic acid (methanol + acetic acid: 30 + 10%, 30 min; 20 + 10%, 1 h; 10 + 5%, 2 h; respectively) at room temperature, the gels were imaged under a Gel Imaging Analysis system (Beijing Liuyi Biotechnology Co., Ltd., Beijing, China) and the band intensities were quantified using Gel-Pro Analyzer software version 4.0 (Media Cybernetics, Inc., Rockville, MD, USA).

Animals. Male apoE$^{-/-}$ mice (6-weeks-old; weight, 20 g; n=24) were purchased from Beijing Vital River Laboratory Animal Technology Co., Ltd. (Beijing, China). The mice were housed in cages (temperature, 22˚C) with a 12-h light/dark cycle and allowed *ad libitum* access to food and water. The protocols of animal experiments were performed following the National Institutes of Health Laboratory Animal Care and Use Guidelines (21) and approved by the Animal Ethics Committee at Jilin University.

Animal model of atherosclerosis. ApoE$^{-/-}$ mice were randomized into the following four groups: Control, Model, siCtr and siADRP. ApoE$^{-/-}$ mice were fed a high-fat diet containing

0.15% cholesterol and 21% fat for 12 weeks to establish the animal model of atherosclerosis. One week after establishment of the mouse model of atherosclerosis, the mice were injected with saline or siCtr/siADRP (5 mg/kg) via the tail vein twice a week for 3 weeks (n=6 per group). ApoE$^{-/-}$ mice fed a standard chow diet served as the control. Following animal experiments, all mice were euthanized by sodium pentobarbital (100 mg/kg body weight; LookChem Co., Ltd., Hangzhou, China) and underwent thoracotomy and the thoracic aortas were exposed and excised. Some aortas were fixed in 4% paraformaldehyde for histological evaluation and some aortas were snap-frozen in liquid nitrogen and stored at -70°C for further analyses.

Hematoxylin and eosin (H&E) staining. The paraformaldehyde-fixed aortas (for 48 h, at room temperature) were dehydrated in gradient ethanol, embedded in paraffin and cut into 5-μm sections. The sections were stained with H&E and imaged under an Olympus DP73 microscope (Olympus Corporation, Tokyo, Japan). The neointima and media areas were measured and the ratio of neointima/media area was calculated as described previously (22).

Reverse transcription-quantitative polymerase chain reaction (RT-qPCR). Total RNA was isolated from mouse aortas using a Total RNA Extraction kit (Tiangen Biotech Co., Ltd., Beijing, China) and cDNA was synthesized using Super M-MLV Reverse Transcriptase (BioTeke Corporation, Beijing, China) according to the protocol described below. The reaction mixture contained 1 μg RNA, 2 μl dNTP (BioTeke Corporation), 1 μl random primer (Sangon Biotech Co., Ltd., Shanghai, China), 1 μl oligo (dT)$_{15}$ (Tiangen Biotech Co., Ltd.) and ddH$_2$O was added to a final volume of 14.5 μl. The reaction was denatured in a 70°C water bath for 5 min, and incubated in an ice bath for 2 min. To perform the RT reaction, 4 μl 5X buffer, 0.5 μl RNasin and 1 μl super M-MLV reverse transcriptase (200 U) was added into the reaction mixture and incubated at 25°C for 10 min, 42°C for 50 min and 95°C for 5 min. The mRNA expression level of ADRP was evaluated using a Real-Time Quantitative PCR system (Bioneer Corporation, Daejeon, Korea) and SYBR-Green I (Beijing Solarbio Science & Technology Co., Ltd., Beijing, China). qPCR conditions consisted of 10 min at 95°C, followed by 10 sec at 95°C, 20 sec at 60°C and 30 sec at 72°C (40 cycles). The relative gene expression was assessed using the $2^{-\Delta\Delta Cq}$ method to normalize expression to β-actin (23). Each experiment was repeated three times. The primer sequences were as follows: ADRP, 5'-AAG AGCCAGGAGACCATT-3' (forward) and 5'-CCACCCACG AGACATAGA-3' (reverse); and β-actin, 5'-TTTTCCAGCCTT CCTTCTTGGGTAT-3' (forward) and 5'-CTGTGTTGGCAT AGAGGTCTTTACG-3' (reverse).

Western blotting. Primary human aortic VMSCs and mice aortic tissues were treated with lysis buffer (Wanleibio) containing 1% PMSF on ice for 5 min to obtain the protein extracts (10,005 x g, 10 min, 4°C) and a BCA assay kit (Wanleibio) was used to determine the protein concentration according to the manufacturer's protocol. Total proteins were boiled with loading buffer, subjected to 8 or 10% SDS-PAGE (40 μg per lane) and transferred onto polyvinylidene fluoride membranes (EMD Millipore, Billerica, MA, USA). After

blocking with 1% bovine serum albumin (Amresco, LLC) or 5% non-fat milk for 1 h at room temperature with gentle shaking, the membranes were incubated with rabbit anti-human polyclonal antibodies against proliferating cell nuclear antigen (PCNA; cat. no. bs-2006R; 1:500; BIOSS, Beijing, China), MMP-2 (cat. no. BA0569; 1:400; Wuhan Boster Biological Technology, Ltd., Wuhan, China), MMP-9 (cat. no. BA0573; 1:400; Wuhan Boster Biological Technology, Ltd.), ERK (cat. no. bs-2637R; 1:500; BIOSS), phosphorylated (p)-ERK (cat. no. bs-1522R; 1:500; BIOSS), Akt (cat. no. sc-8312; 1:500; Santa Cruz Biotechnology, Inc., Dallas, Texas, USA), p-Akt (cat. no. sc-135651; 1:500; Santa Cruz Biotechnology, Inc.), ADRP (cat. no. bs-1164R; 1:500; BIOSS) and β-actin (cat. no. sc-47778; 1:1,000; Santa Cruz Biotechnology, Inc.) at 4°C overnight, followed by incubation with a horseradish peroxidase-conjugated goat anti-rabbit/mouse secondary antibody (cat. no. WLA023/WLA024; 1:5,000; Wanleibio) at 37°C for 45 min. β-actin served as an internal control. The protein bands were visualized using Enhanced Chemilumiescence reagent (Wanleibio) and quantified by Gel-Pro Analyzer software version 4.0 (Media Cybernetics, Inc., Rockville, MD, USA). Each experiment was repeated three times.

Statistical analysis. Data are presented as the mean ± standard deviation. Statistical analyses were performed using one-way analysis of variance followed by Bonferroni's post hoc test using GraphPad Prism software version 5.0 (GraphPad Software, Inc., La Jolla, CA, USA). P<0.05 was considered to indicate a statistically significant difference.

Results

ADRP knockdown attenuates PDGF-induced proliferation of human VSMCs. VSMCs were transfected with or without siCtr/siADRP and treated with 10 ng/ml PDGF. Cell viability was examined by MTT assay. The results demonstrated that PDGF increased VSMC viability at 24, 48 and 72 h, compared with the control group (Fig. 1A). However, ADRP knockdown significantly inhibited the increases in VSMC viability induced by PDGF incubation at 72 h. Furthermore, the present study analyzed the cell cycle distribution in VSMCs. It was observed that the G1-phase cell population in the PDGF group was significantly lower compared with the control group (Fig. 1B). The cell percentage at S-phase in the PDGF group was significantly higher compared with the control group. However, in the presence of PDGF, siADRP significantly increased G1-phase cell population and decreased the cell population at S-phase and G2-phase (Fig. 1B). The expression level of proliferation marker PCNA was confirmed by western blotting (Fig. 1C). PDGF significantly increased PCNA protein expression levels compared with control cells, while ADRP knockdown attenuated PDGF-stimulated elevation of PCNA expression (Fig. 1C).

ADRP knockdown inhibits PDGF-stimulated migration of VSMCs. The present study further examined the effect of ADRP knockdown on cell migration by performing a wound healing assay. As presented in Fig. 2A, PDGF significantly promoted wound closure at 12 and 24 h after the scratch, whereas knockdown of ADRP exhibited an inhibitory effect
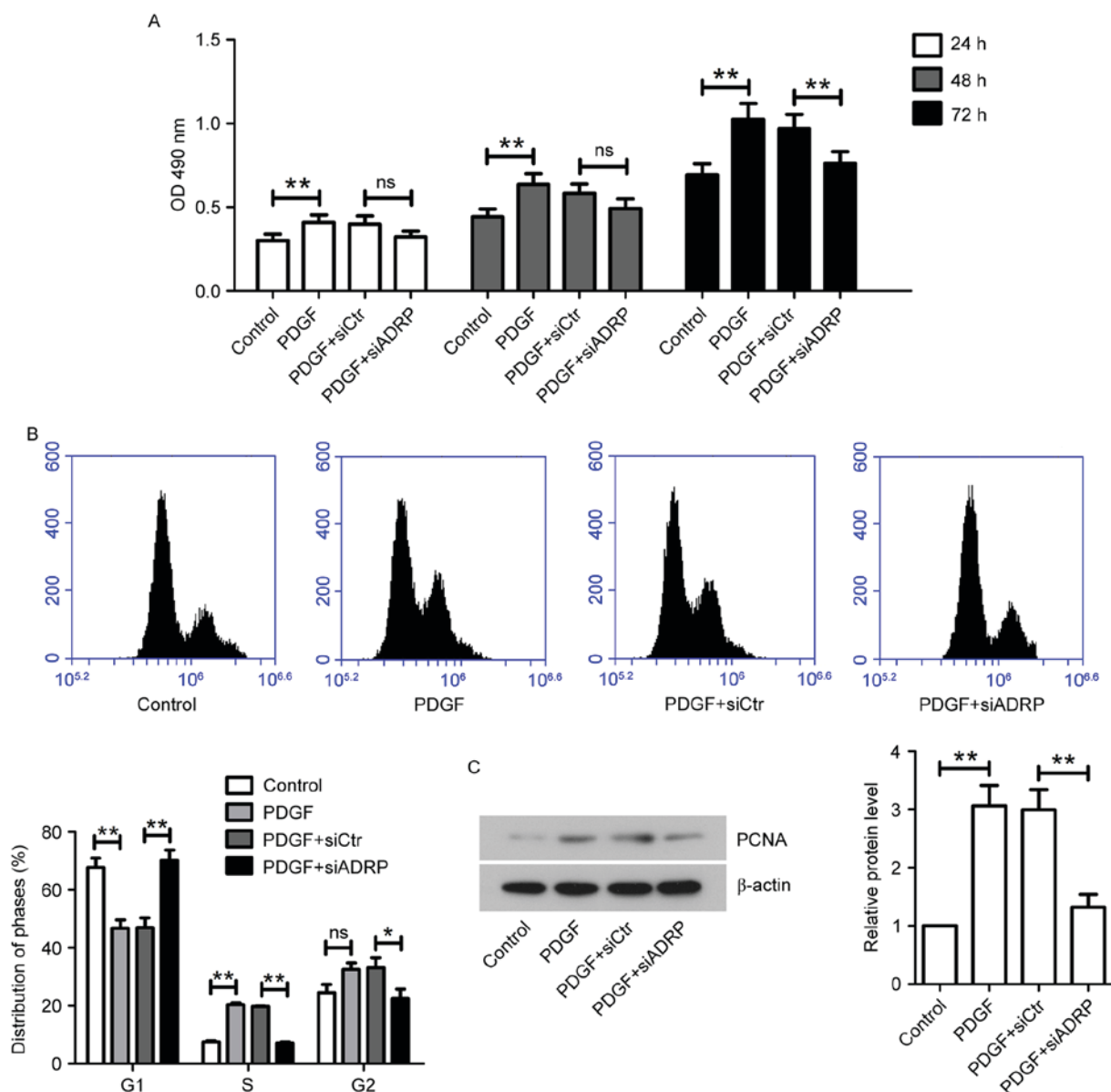
Figure 1. Effect of ADRP knockdown on VSMC viability and cell cycle progression induced by PDGF. (A) At 24 h after transfection with siCtr or siADRP, VSMCs were stimulated with 10 ng/ml PDGF. Cell viability was measured by MTT assay at 24, 48 and 72 h. The absorbance at 490 nm was measured. VSMCs were incubated for 48 h with PDGF at 24 h post-transfection. Cell cycle distribution was analyzed by (B) flow cytometry and PCNA protein expression was quantified by (C) western blotting. β-actin served as an internal control. Data are presented as the mean ± standard deviation. *P<0.05 and **P<0.01. ADRP, adipose differentiation-related protein; VSMCs, vascular smooth muscle cells; PDGF, platelet-derived growth factor; siRNA, small interfering RNA; siCtr, control siRNA; siADRP, siRNA targeting ADRP; PCNA, proliferating cell nuclear antigen; OD, optical density.

on PDGF-induced migration of VSMCs. This inhibitory effect on cell migration was further confirmed by the Transwell migration assay (Fig. 2B). MMP-2 and MMP-9 are critical for tissue remodeling and cell migration (24). Therefore, the effect of ADRP knockdown on MMP-2 and MMP-9 in cells exposed to PDGF was examined using western blotting (Fig. 2C) and gelatin zymography (Fig. 2D). The results indicated that PDGF increased the expression and activities of MMP-2 and MMP-9 in VSMCs compared with control cells, while ADRP knockdown significantly decreased PDGF-induced upregulation of MMP-2 and MMP-9 levels and activities.

ADRP knockdown inhibits the ERK and Akt signaling pathways. Accumulating evidence has demonstrated that the ERK and Akt signaling pathways are involved in the proliferation

and migration of VSMCs (25,26). However, whether ADRP knockdown inhibits VSMC proliferation and migration via the ERK and Akt pathways remains to be established. Western blotting results demonstrated that the ratios of p-ERK/ERK and p-Akt/Akt in VSMCs were decreased by ADRP knockdown, despite the presence of PDGF (Fig. 3).

ADRP knockdown attenuates neointima formation in a mouse model of atherosclerosis. To investigate the effect of ADRP on neointima formation *in vivo*, animal models of atherosclerosis were administrated with siCtr or siADRP twice a week for 3 weeks, and aortas were obtained. The mRNA and protein expression of ADRP in the aortas was examined at the end of the animal experiments. The results demonstrated that ADRP mRNA and protein expression was
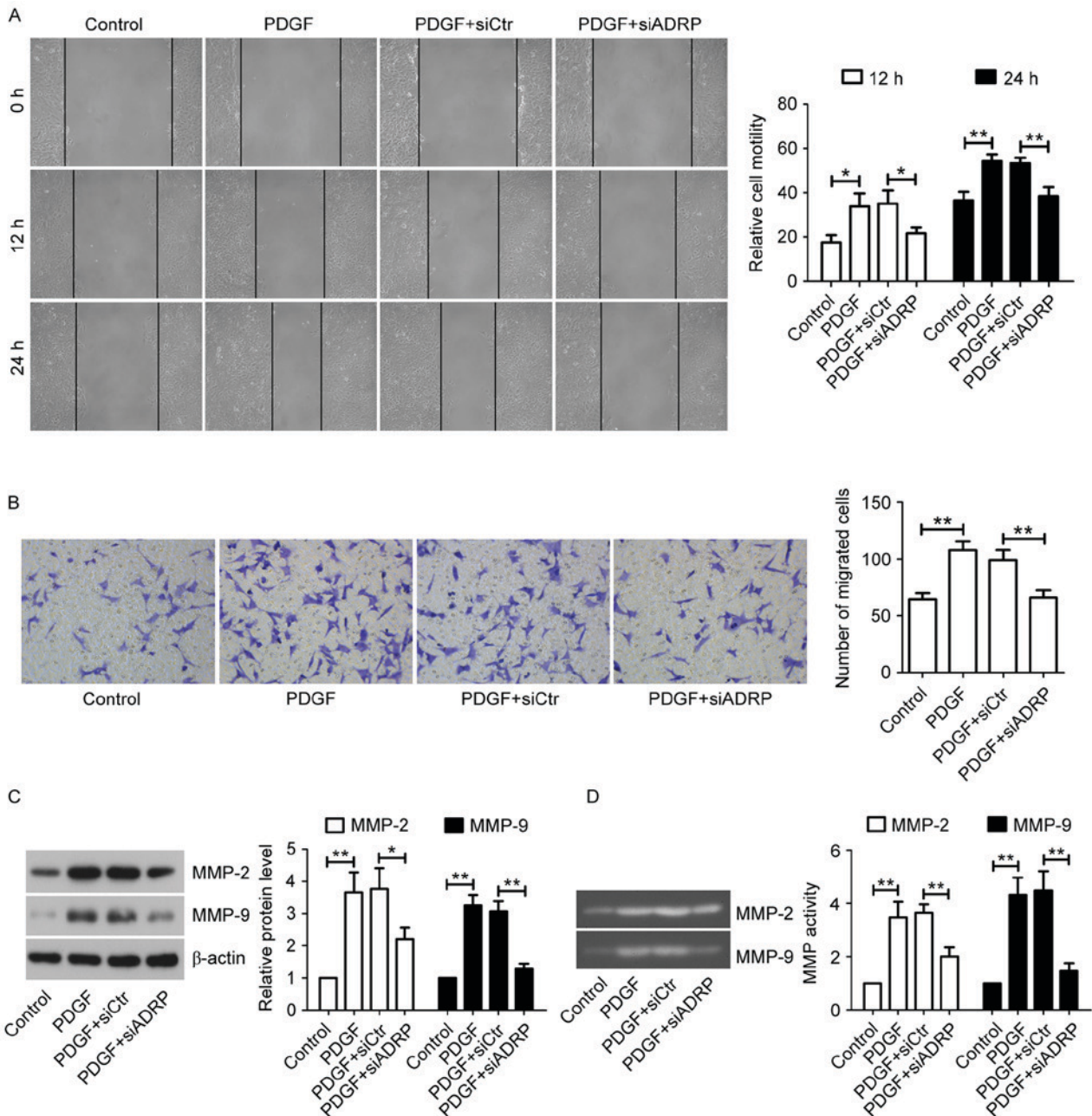
Figure 2. Effect of ADRP knockdown on VSMC migration induced by PDGF. (A) Cell migration was determined by wound healing assay at 12 and 24 h (magnification, x100). (B) Cell migration ability was confirmed by Transwell migration assay (magnification, x200). VSMCs were incubated for 24 h with PDGF at 24 h post-transfection. The protein levels and activities of MMP-2 and MMP-9 were examined by (C) western blotting and (D) gelatin zymography. Data are presented as the mean ± standard deviation. *P<0.05 and **P<0.01, as indicated by brackets. ADRP, adipose differentiation-related protein; VSMCs, vascular smooth muscle cells; PDGF, platelet-derived growth factor; MMP, matrix metalloproteinase; siRNA, small interfering RNA: siCtr, control siRNA; siADRP, siRNA targeting ADRP.

significantly increased in model mice compared with controls (Fig. 4A and B). However, elevated ADRP expression was significantly reduced by siADRP injection, as indicated by RT-qPCR and western blotting. In addition, neointima formation was assessed using H&E staining. The results indicated that the model mice exhibited a reduced lumen area and increased neointima area, and neointima/media area ratio, when compared with control mice (Fig. 4C). However, the lumen area was significantly increased and the ratio of neointima/media area was significantly decreased in the aortas of the siADRP-treated mice compared with siCtr-treated mice (Fig. 4C).

Discussion

In the present study, ADRP was silenced in VSMCs using siRNA. The results demonstrated that ADRP knockdown inhibited PDGF-induced proliferation and migration of VSMCs by inhibiting the ERK and Akt signaling pathways. In addition, apoE$^{-/-}$ mice were used to establish an animal model of atherosclerosis in order to examine the effect of ADRP knockdown on atherosclerosis in vivo. The results indicated that ADRP knockdown inhibited neointima formation in mice.

Abnormal proliferation of VSMCs is key to the development of atherosclerosis (27). It has been widely demonstrated
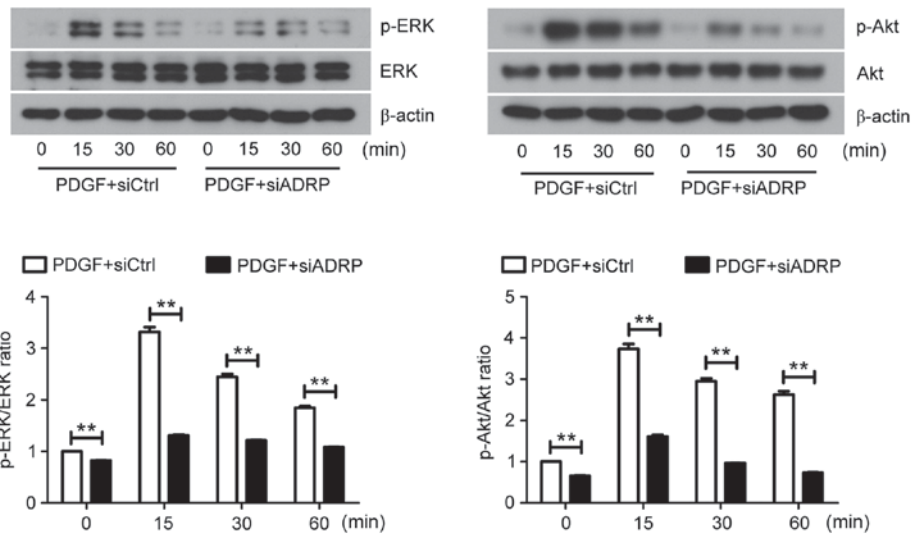
Figure 3. Effect of ADRP knockdown on the ERK and Akt signaling pathways. At 48 h after siRNA transfection, VSMCs were exposed to PDGF for 0, 15, 30 and 60 min. The protein expression of ERK, p-ERK, Akt and p-Akt was subsequently examined by western blotting. Representative images are presented. Data are presented as the mean ± standard deviation. $^{**}P<0.01$, as indicated by brackets. ADRP, adipose differentiate-related protein; ERK, extracellular signal-regulated kinase; siRNA, small interfering RNA; VSMCs, vascular smooth muscle cells; PDGF, platelet-derived growth factor; p-, phosphorylated; siCtrl, control siRNA; siADRP, siRNA targeting ADRP.
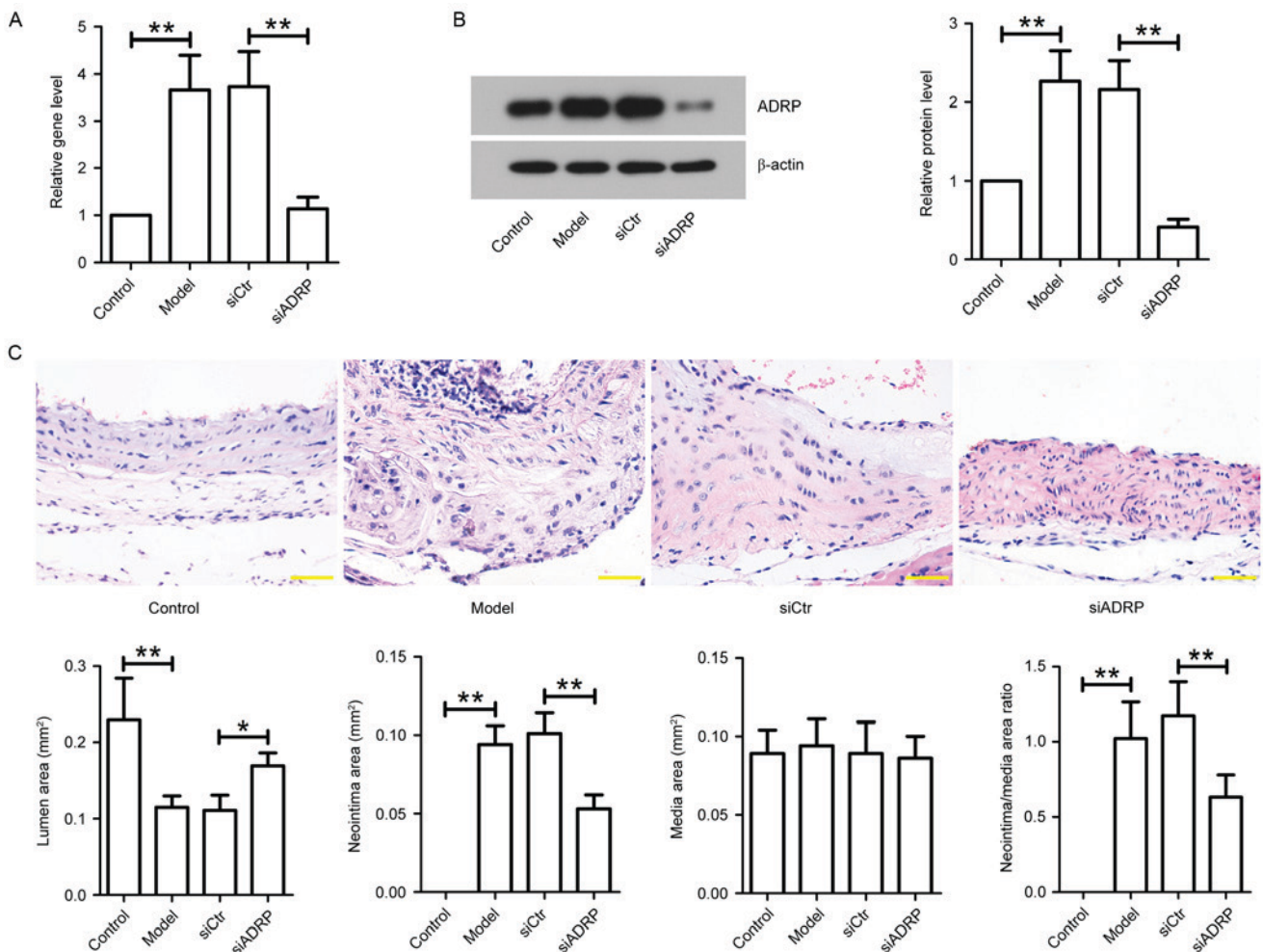

Figure 4. Effect of ADRP knockdown on neointima formation in apoE$^{-/-}$ mice. After establishing an *in vivo* model of atherosclerosis, the mice were injected with siCtr or siADRP twice a week. After 3 weeks of siRNA injection, aortas were obtained. (A) ADRP mRNA levels were examined by reverse transcription-quantitative polymerase chain reaction. (B) ADRP protein levels were determined by western blotting. β-actin served as an internal control. (C) Aortas were subjected to hematoxylin and eosin staining, and lumen area, neointima area, media area and neointima/media area ratios were measured to evaluate neointima formation in mice. Scale bar, 50 µm. Data are presented as the mean ± standard deviation. $^{*}P<0.05$ and $^{**}P<0.01$, as indicated by brackets. ADRP, adipose differentiation-related protein; apoE, apolipoprotein E; siRNA, small interfering RNA; siCtr, control siRNA; siADRP, siRNA targeting ADRP.

that multiple growth factors and cytokines, including PDGF, contribute to the abnormal proliferation of VSMCs (28,29). ADRP is a major lipid-droplet protein. It regulates the formation of foam cells from macrophages and has an important role in the development of atherosclerosis (12,30). However, to the best of our knowledge, no previous studies have investigated the effect of ADRP knockdown on the proliferation of VSMCs induced by PDGF. The present study demonstrated that ADRP knockdown inhibited PDGF-induced growth and proliferation of VSMCs, and that this anti-proliferative effect was associated with increased cell cycle arrest at G1 phase. Cell proliferation is controlled by cell cycle progression, which is regulated by the complexes of cyclins and cyclin-dependent kinases (31). PCNA is a cell cycle protein in the nucleus and functions in DNA synthesis (32). PCNA is commonly used as a marker to assess the state of cell proliferation (33). The results of the current study demonstrated that ADRP silencing decreased the expression level of PCNA in PDGF-treated VSMCs. These results indicated that the inhibitory effect of ADRP knockdown on cell proliferation may be due to cell cycle arrest at G1 phase and the downregulation of PCNA expression.

A previous study demonstrated that migration of VSMCs is also involved in the progression of cardiovascular diseases, such as atherosclerosis (34). The proliferative and migratory activities can be enhanced by growth promoters such as PDGF (35). However, the effect of ADRP knockdown on PDGF-treated VSMCs remains unknown. The current study also assessed the migration of VSMCs using wound healing and Transwell migration assays. The results demonstrated that PDGF-stimulated VSMC migration was inhibited by knockdown of ADRP. MMPs belong to the zinc-dependent proteinase family (36). During VSMC migration, MMPs are secreted to degrade extracellular matrix proteins and the vascular basement membrane (35,37). A recent study reported that MMP-2 and MMP-9 are associated with the pathogenesis of atherosclerosis, and the levels of MMPs are upregulated in atherosclerotic plaques (34). In the present study, ADRP knockdown significantly decreased MMP-2 and MMP-9 levels and activities in PDGF-stimulated VSMCs. The results indicated that ADRP silencing suppresses VSMC migration by regulating the expression and activities of MMP-2 and MMP-9.

PDGF binds with its receptor and subsequently activates various intracellular signaling pathways, including signal transducer and activator of transcription, ERK/MAPK and phosphatidylinositol 3-kinase/Akt, which contribute to VSMC proliferation and migration (27,38). However, whether ADRP regulates the proliferation and migration of VSMCs via the ERK and Akt pathways remains unclear. After silencing ADRP expression using siADRP in the current study, it was observed that ADRP knockdown inhibited the phosphorylation of ERK and Akt in PDGF-treated VSMCs. These results indicate that ADRP silencing may suppress proliferation and migration of VSMCs by inhibiting ERK and Akt signaling pathways.

Apolipoprotein E (apoE) is a primary apolipoprotein and functions in maintaining cholesterol balance and lipid metabolism (39). ApoE$^{-/-}$ mice are susceptible to atherosclerosis and have been widely used to induce atherosclerosis (40). Previous studies have reported that ADRP overexpression induces foam cell formation, and ADRP deficiency attenuates atherogenesis by impairing the formation of foam cells (13,41). In the present study, siADRP administration significantly decreased ADRP mRNA and protein expression levels in aortas of apoeE$^{-/-}$ mice. The current study subsequently assessed the effect of ADRP knockdown on neointima formation in apoE$^{-/-}$ mice. Neointima formation, characterized by thickening of intimal layer, is involved in various diseases, including atherosclerosis and angioplasty (42). The results demonstrated that ADRP silencing significantly increased the lumen area, and decreased the neointima area and neointima/media area ratio in vascular tissues, as determined by H&E staining.

In conclusion, the present study demonstrated that ADRP knockdown significantly inhibited PDGF-induced proliferation and migration of VSMCs and arrested the cell cycle at G1 phase, accompanied with inhibition of the ERK and Akt signaling pathways. In the *in vivo* study, the results indicated that knockdown of ADRP suppressed neointima formation in apoE$^{-/-}$ mice. Therefore, ADRP may represent a promising target for the treatment of atherosclerosis.

References

1. Cheng HY, Gaddis DE, Wu R, McSkimming C, Haynes LD, Taylor AM, McNamara CA, Sorci-Thomas M and Hedrick CC: Loss of ABCG1 influences regulatory T cell differentiation and atherosclerosis. J Clin Invest 126: 3236-3246, 2016.
2. Mathur P, Ding Z, Saldeen T and Mehta JL: Tocopherols in the prevention and treatment of atherosclerosis and related cardiovascular disease. Clin Cardiol 38: 570-576, 2015.
3. Su G, Sun G, Liu H, Shu L, Zhang J, Guo L, Huang C and Xu J: Niacin suppresses progression of atherosclerosis by inhibiting vascular inflammation and apoptosis of vascular smooth muscle cells. Med Sci Monit 21: 4081-4089, 2015.
4. Li T, Li D, Xu H, Zhang H, Tang D and Cao H: Wen-Xin Decoction ameliorates vascular endothelium dysfunction via the PI3K/AKT/eNOS pathway in experimental atherosclerosis in rats. BMC Complement Altern Med 16: 27, 2016.
5. Abu-Fanne R, Maraga E, Abd-Elrahman I, Hankin A, Blum G, Abdeen S, Hijazi N, Cines DB and Higazi AA: α-Defensins induce a post-translational modification of low density lipoprotein LDL that promotes atherosclerosis at normal levels of plasma cholesterol. J Biol Chem 291: 2777-2786, 2016.
6. Kim HJ: Role of nucleotide-binding and oligomerization domain 2 protein (NOD2) in the development of atherosclerosis. Korean J Physiol Pharmacol 19: 479-484, 2015.
7. Zhai H, Chen QJ, Gao XM, Ma YT, Chen BD, Yu ZX, Li XM, Liu F, Xiang Y, Xie J and Yang YN: Inhibition of the NF-κB pathway by R65 ribozyme gene via adeno-associated virus serotype 9 ameliorated oxidized LDL induced human umbilical vein endothelial cell injury. Int J Clin Exp Pathol 8: 9912-9921, 2015.
8. Zhou Y, Zhang MJ, Li BH, Chen L, Pi Y, Yin YW, Long CY, Wang X, Sun MJ, Chen X, *et al*: PPARγ inhibits VSMC proliferation and migration via attenuating oxidative stress through upregulating UCP2. PLoS One 11: e0154720, 2016.
9. Liu F, Wang C, Zhang L, Xu Y, Jang L, Gu Y, Cao X, Zhao X, Ye J and Li Q: Metformin prevents hepatic steatosis by regulating the expression of adipose differentiation-related protein. Int J Mol Med 33: 51-58, 2014.
10. McIntosh AL, Senthivinayagam S, Moon KC, Gupta S, Lwande JS, Murphy CC, Storey SM and Atshaves BP: Direct interaction of Plin2 with lipids on the surface of lipid droplets: A live cell FRET analysis. Am J Physiol Cell Physiol 303: C728-C742, 2012.
11. Magne J, Aminoff A, Perman Sundelin J, Mannila MN, Gustafsson P, Hultenby K, Wernerson A, Bauer G, Listenberger L, Neville MJ, *et al*: The minor allele of the missense polymorphism Ser251Pro in perilipin 2 (PLIN2) disrupts an α-helix, affects lipolysis, and is associated with reduced plasma triglyceride concentration in humans. FASEB J 27: 3090-3099, 2013.
12. Xu B, Zhao H, Wang S, Sun X and Qin X: Increased ADRP expression in human atherosclerotic lesions correlates with plaque instability. Int J Clin Exp Med 8: 5414-5421, 2015.

13. Paul A, Chang BH, Li L, Yechoor VK and Chan L: Deficiency of adipose differentiation-related protein impairs foam cell formation and protects against atherosclerosis. Circ Res 102: 1492-1501, 2008.
14. Wei L, Li Y and Suo Z: TSPAN8 promotes gastric cancer growth and metastasis via ERK MAPK pathway. Int J Clin Exp Med 8: 8599-8607, 2015.
15. Park SL, Hwang B, Lee SY, Kim WT, Choi YH, Chang YC, Kim WJ and Moon SK: p21WAF1 Is required for inter-leukin-16-induced migration and invasion of vascular smooth muscle cells via the p38MAPK/Sp-1/MMP-9 pathway. PLoS One 10: e0142153, 2015.
16. Xu T, Zhu H, Li D, Lang Y, Cao L, Liu Y, Wu W and Chen D: Luteolin inhibits angiotensin II-stimulated VSMC proliferation and migration through downregulation of Akt phosphorylation. Evid Based Complement Alternat Med 2015: 931782, 2015.
17. Liu W, Bagaitkar J and Watabe K: Roles of AKT signal in breast cancer. Front Biosci 12: 4011-4019, 2007.
18. Yang SW, Lim L, Ju S, Choi DH and Song H: Effects of matrix metalloproteinase 13 on vascular smooth muscle cells migration via Akt-ERK dependent pathway. Tissue Cell 47: 115-121, 2015.
19. Yu X, Li Z, Chen G and Wu WK: MicroRNA-10b induces vascular muscle cell proliferation through Akt pathway by targeting TIP30. Curr Vasc Pharmacol 13: 679-686, 2015.
20. He M, Xue ZM, Li J and Zhou BQ: Breviscapine inhibits high glucose-induced proliferation and migration of cultured vascular smooth muscle cells of rats via suppressing the ERK1/2 MAPK signaling pathway. Acta Pharmacol Sin 33: 606-614, 2012.
21. Institute of Laboratory Animal Resources: Guide for the Care and Use of Laboratory Animals. National Academy Press, Washington, DC, 1996.
22. Kumar A, Hoover JL, Simmons CA, Lindner V and Shebuski RJ: Remodeling and neointimal formation in the carotid artery of normal and P-selectin-deficient mice. Circulation 96: 4333-4342, 1997.
23. Livak KJ and Schmittgen TD: Analysis of relative gene expression data using real-time quantitative PCR and the 2(-Delta Delta C(T)) Method. Methods 25: 402-408, 2001.
24. Zhang Y, George J, Li Y, Olufade R and Zhao X: Matrix metal-loproteinase-9 expression is enhanced in renal parietal epithelial cells of zucker diabetic fatty rats and is induced by albumin in in vitro primary parietal cell culture. PLoS One 10: e0123276, 2015.
25. Guo J, Li L, Wu YJ, Yan Y, Xu XN, Wang SB, Yuan TY, Fang LH and Du GH: Inhibitory effects of Brazilin on the vascular smooth muscle cell proliferation and migration induced by PDGF-BB. Am J Chin Med 41: 1283-1296, 2013.
26. Park ES, Kang SI, Yoo KD, Lee MY, Yoo HS, Hong JT, Shin HS, Kim B and Yun YP: Camptothecin inhibits platelet-derived growth factor-BB-induced proliferation of rat aortic vascular smooth muscle cells through inhibition of PI3K/Akt signaling pathway. Exp Cell Res 319: 982-991, 2013.
27. Li PC, Sheu MJ, Ma WF, Pan CH, Sheu JH and Wu CH: Anti-restenotic roles of dihydroaustrasulfone alcohol involved in inhibiting PDGF-BB-stimulated proliferation and migration of vascular smooth muscle cells. Mar Drugs 13: 3046-3060, 2015.
28. Han JH, Lee SG, Jung SH, Lee JJ, Park HS, Kim YH and Myung CS: Sesamin inhibits PDGF-Mediated proliferation of vascular smooth muscle cells by upregulating p21 and p27. J Agric Food Chem 63: 7317-7325, 2015.
29. Yan G, Wang Q, Hu S, Wang D, Qiao Y, Ma G, Tang C and Gu Y: Digoxin inhibits PDGF-BB-induced VSMC proliferation and migration through an increase in ILK signaling and attenuates neointima formation following carotid injury. Int J Mol Med 36: 1001-1011, 2015.
30. Wang J, Si Y, Wu C, Sun L, Ma Y, Ge A and Li B: Lipopolysaccharide promotes lipid accumulation in human adventitial fibroblasts via TLR4-NF-κB pathway. Lipids Health Dis 11: 139, 2012.
31. Gu Y, Chen X, Shang C, Singh K, Barzegar M, Mahdavian E, Salvatore BA, Jiang S and Huang S: Fusarochromanone induces G1 cell cycle arrest and apoptosis in COS7 and HEK293 cells. PLoS One 9: e112641, 2014.
32. Poosarla C, Ramesh M, Ramesh K, Gudiseva S, Bala S and Sundar M: Proliferating cell nuclear antigen in premalig-nancy and oral squamous cell carcinoma. J Clin Diagn Res 9: ZC39-ZC41, 2015.
33. Xie M, Bu P, Li F, Lan S, Wu H, Yuan L and Wang Y: Neonatal bisphenol A exposure induces meiotic arrest and apoptosis of spermatogenic cells. Oncotarget 7: 10606-10615, 2016.
34. Shih MF, Pan KH and Cherng JY: Possible mechanisms of Di(2-ethylhexyl) phthalate-induced MMP-2 and MMP-9 expression in A7r5 Rat vascular smooth muscle cells. Int J Mol Sci 16: 28800-28811, 2015.
35. Rudijanto A: The role of vascular smooth muscle cells on the pathogenesis of atherosclerosis. Acta Med Indones 39: 86-93, 2007.
36. Aroui S, Aouey B, Chtourou Y, Meunier AC, Fetoui H and Kenani A: Naringin suppresses cell metastasis and the expression of matrix metalloproteinases (MMP-2 and MMP-9) via the inhibition of ERK-P38-JNK signaling pathway in human glioblastoma. Chem Biol Interact 244: 195-203, 2016.
37. Ge X, Chen S, Liu M, Liang T and Liu C: Evodiamine attenuates PDGF-BB-Induced migration of rat vascular smooth muscle cells through activating PPARγ. Int J Mol Sci 16: 28180-28193, 2015.
38. Chen S, Liu B, Kong D, Li S, Li C, Wang H and Sun Y: Atorvastatin calcium inhibits phenotypic modulation of PDGF-BB-induced VSMCs via down-regulation the Akt signaling pathway. PLoS One 10: e0122577, 2015.
39. Zhu XJ, Chen LH and Li JH: The effects of aerobic exercise on plasma adiponectin level and adiponectin-related protein expression in myocardial tissue of ApoE(-/-) mice. J Sports Sci Med 14: 877-882, 2015.
40. Getz GS and Reardon CA: ApoE knockout and knockin mice: The history of their contribution to the understanding of athero-genesis. J Lipid Res 57: 758-766, 2016.
41. Feng X, Yuan Y, Wang C, Feng J, Yuan Z, Zhang X, Sui W, Hu P, Zheng P and Ye J: Autophagy involved in lipopolysac-charide-induced foam cell formation is mediated by adipose differentiation-related protein. Lipids Health Dis 13: 10, 2014.
42. Huang L, Zhang SM, Zhang P, Zhang XJ, Zhu LH, Chen K, Gao L, Zhang Y, Kong XJ, Tian S, *et al*: Interferon regulatory factor 7 protects against vascular smooth muscle cell proliferation and neointima formation. J Am Heart Assoc 3: e001309, 2014.